Single-particle diffusion in dense inhomogeneous colloid suspensions in ribbon channels

Emily Wonder, Binhua Lin,* and Stuart A. Rice*

Department of Chemistry, CARS and The James Franck Institute, The University of Chicago, Chicago, Illinois 60637, USA

(Received 15 June 2011; revised manuscript received 21 September 2011; published 18 October 2011)

We report the results of a study of single-particle diffusion in dense colloid fluids confined in a ribbon channel geometry that is intermediate between quasione dimensional (q1D) and quasitwo dimensional (q2D). This paper complements a previous paper about pair diffusion in the same system [Phys. Rev. E **82**, 031403 (2010)]. In all of the systems studied, the colloid density distribution transverse to the ribbon channel is stratified with peak amplitudes that depend on the colloid density. Although the virtual walls that confine a stratum are structured with a scale length of the colloid diameter, that structure does not have an apparent influence on the single-particle diffusion, which shows the characteristic features of diffusion in a q1D channel with smooth walls. We find that, for all channel widths and packing fractions studied, the single-particle transverse diffusion coefficient in a stratum is smaller than the single-particle longitudinal diffusion coefficient in the same stratum and that the single-particle longitudinal diffusion coefficient varies very little from stratum to stratum, being only slightly smaller in the dense strata next to the walls than in the central strata. The lack of variation in the longitudinal diffusion coefficient with apparent stratum density is explained by the application of the Fischer-Methfessel approximation to the local density in an inhomogeneous liquid. The ratio of the transverse to longitudinal diffusion coefficients varies very slowly with ribbon width, implying a very slow transition from q1D to q2D behavior.

DOI: 10.1103/PhysRevE.84.041403 PACS number(s): 82.70.−y, 66.10.C−, 47.57.J−

I. INTRODUCTION

Interest in the effects of confinement on the particle dynamics and the hydrodynamic interactions in dense colloid fluids has attracted considerable attention in the last decade, driven, in part, by fundamental questions concerning the influence of dimensionality on the transport properties of a system and, in part, by the practical applications of confined colloid suspensions [1–3]. A survey of the relationships between structure, confinement, and particle-particle interaction can be found in Ref. [4].

We recently reported studies of the density distribution and the transverse and longitudinal pair-diffusion coefficients in colloid suspensions confined in ribbon channels whose width varies from about 2 to 12 colloid diameters, a geometry that is intermediate between q1D and q2D [5,6]. The main structural feature of such a system is that the density distribution of the fluid transverse to the ribbon walls is stratified, which also has been observed in three-dimensional (3D) colloid suspensions near a wall or narrowly confined between two smooth walls [7–9]. We consider a system to have a quasi-one-dimensional (q1D) character if the channel that confines it is less than two particle diameters wide and to have a quasi-two-dimensional (q2D) character if it is confined between two smooth walls separated by less than two particle diameters. In the q1D system, the mean positions of the centers of the colloid particle lie on a line, but small displacements perpendicular to the line occur. In the q2D system, the mean positions of the centers of the colloid particle lie in a plane, but small displacements perpendicular to the plane occur. In both the q1D and q2D systems, one particle cannot pass another via motion perpendicular to the line or plane of centers.

The focus of our previous papers was on the transition between q1D and q2D behavior in dense colloid suspensions, using the ribbon channels as a vehicle. We found that the order along the strata is characteristic of a q1D liquid, even at a density near to close packing [6]. However, if the stratified density distribution is ignored, the order on the length scale of the width of the channel is characteristic of a q2D liquid or solid, supporting the view that ribbon suspensions fall into the unknown domain between q1D and q2D geometries. The dynamics of the colloid motion in the ribbon systems, examined with pair-diffusion coefficients (that is, via the influence of hydrodynamic couplings between a pair of colloid particles), are found to be multifaceted [5]. While the hydrodynamic coupling already exhibits q2D characteristics for relatively narrow channels when measured along the channel's axis, it continues to deviate from the expected q2D behavior even for the widest channels studied when it is measured transverse to the channel axis. Furthermore, colloids within each stratum behave as if they are confined in q1D geometry.

In this short paper, we again examine the transition between q1D and q2D behavior in colloid suspensions confined in ribbon channels, focusing attention on the one-particle diffusion coefficient. Our motivation for doing so is contained in three questions relevant to the q1D to q2D transition that are not addressed by our previous paper. First, given the stratification of the density distribution transverse to the ribbon channel, does the corrugation of the nearest neighboring strata affect the short-time single-particle diffusion coefficient? Second, does the short-time single-particle diffusion coefficient vary from stratum to stratum across the channel, and/or from peak to trough of the density distribution? Third, if the stratification of the transverse density distribution in the ribbon channel is disregarded, by averaging over all the strata in the channel, how does the single-particle diffusion coefficient for the confined suspension differ from that in an infinite q2D suspension?

*blin@uchicago.edu; sarice@uchicago.edu

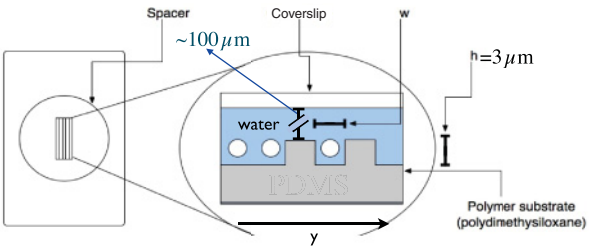

FIG. 1. (Color online) Schematics of a ribbon channel.

II. EXPERIMENTAL DETAILS

Detailed sample preparation and data processing procedures have been described in our previous paper on the equilibrium structure and pair diffusion in the same colloid suspensions and ribbon channels [5,6]. Briefly, our experimental system consists of a sample cell that contains a single layer of a silica spherical colloid suspension(Duke Scientific, $\sigma = 1.58 \pm 0.04$ μm, density 2.2 g/cm^3) confined to long narrow channels of various widths w but the same depth h ($h = 3$ μm). The channels were printed on a polydimethysiloxane (PDMS) substrate from a master pattern fabricated lithographically (Stanford Nanofabrication Facility). A diagram of the experimental arrangement and images of the colloids in the ribbon channels are displayed in Fig. 1. Digital video microscopy was used to extract time-dependent 2D trajectories of the colloid particles (with a time resolution of 0.033 s), and the short-time domain within which the in-stratum diffusion coefficient was obtained was $0.033 < t < 0.2$ s.

The data for the ribbon channels were compared with those for the q1D and q2D geometries, which were obtained using the same colloid preparation. In the case of the q1D geometry, at each density, a single file of the same silica spheres was confined in a channel whose width and depth were 3 μm [10]; in the case of the q2D geometry, at each density, a single layer of the same silica spheres was confined between two hard walls whose gap was 1.7 μm [11].

We note that the ribbon channels are unconfined at the top. Nevertheless, the microscope images show that the colloid particle centers lie in the focal plane and remain there for the duration of the experiments. We rarely observe jumping of particles out of or into the ribbon channel. Furthermore, as shown in earlier studies of colloid suspensions in q1D channels that are unconfined at the top [10], the influence of hydrodynamic interactions is well accounted for when the channel is represented as a fully closed capillary with the effective radius very close to the channel width (and depth). Put another way, because the fluid in the q1D channel and above are quiescent, there must be a boundary in the fluid that contacts the lips of the channel and on which the fluid velocity vanishes. We assume that the same situation exists for the ribbon channels.

The particle density distributions in all samples in the ribbon channels were uniform along the x axis (the direction of the channel). However, the extent of particle displacement transverse to the channel (y direction) is less than the width of the channel. We attribute this to the nonwetting property of the PDMS wall. The effective width of the channel $w_{\rm eff}$ is approximately 1 μm less than w along each wall as calculated from the histogram of the colloid particle positions and the distance between the most widely separated density peaks. We assume, likewise, that the effective depth of all the channels is $h_{\rm eff} \approx 2$ μm. For clarity, the experimental data sets will be referred to using the fabricated channel width w. The packing fraction was calculated using $\phi = N\pi\sigma^2/4lw_{\rm eff}$ with l as the length of the channel in the field of view (108 μm) and N as the average number of particles in the viewed section of the channel. The transverse density distribution in the ribbon channel was separated into strata centered on the peaks with widths defined by the minima in the distribution. The single-particle diffusion coefficient along (longitudinal) and perpendicular (transverse) to each stratum was calculated from the variation of the mean square displacement with time. The values reported for the diffusion coefficients refer to the short-time linear regime wherein the mean square displacement is proportional to time.

III. RESULTS AND DISCUSSION

We first address questions 1 and 2 from Sec. I using the experimental results shown in Figs. 2–4.

In Fig. 2, we display samples of the in-stratum short-time single-particle diffusion coefficients for ribbon channels with widths of 5 μm [Fig. 2(a)], 8 μm [Fig. 2(b)], 11 μm [Fig. 2(c)], 14 μm [Fig. 2(d)], and 20 μm [Fig. 2(e)], all with packing fraction $\phi \approx 0.4$. The figure shows a superposition of the transverse density profile in the ribbon channel $P(y)$ and the short-time single-particle diffusion coefficients along and perpendicular to the strata of the transverse density distribution. The diffusion coefficient data, also listed in Table I, are for the strata in the density profile shown by the symbols. The dominant qualitative features of the data, for all packing fractions, are the following:

(1) For all channel widths and packing fractions studied, the single-particle transverse diffusion coefficient in a stratum is smaller than the single-particle longitudinal diffusion coefficient in the same stratum.

(2) The single-particle longitudinal diffusion coefficient varies very little from stratum to stratum, being only slightly smaller in the dense strata next to the walls than in the central strata. The single-particle transverse diffusion coefficient is much smaller in the dense strata next to the walls than in the central strata but varies little in the central strata.

(3) For the widest channel and highest density studied (20-μm channel with packing fraction $\phi \approx 0.41$), the transverse density distribution has very distinct peaks near the walls and is nearly uniform in the central region. We subdivide this transverse density distribution into equal width strata centered on the maxima and minima of the distribution and determine the corresponding diffusion coefficients. As shown in Fig. 3, both the single-particle longitudinal and the transverse diffusion coefficients are sensibly the same for strata centered on the minima and maxima of the density distribution, except for the strata closest to the walls of the channel.

(4) There is a small variation across the inner strata of the density distribution of the ratio of the single-particle transverse to longitudinal diffusion coefficients. That ratio is larger for the central stratum than for the surrounding strata. The

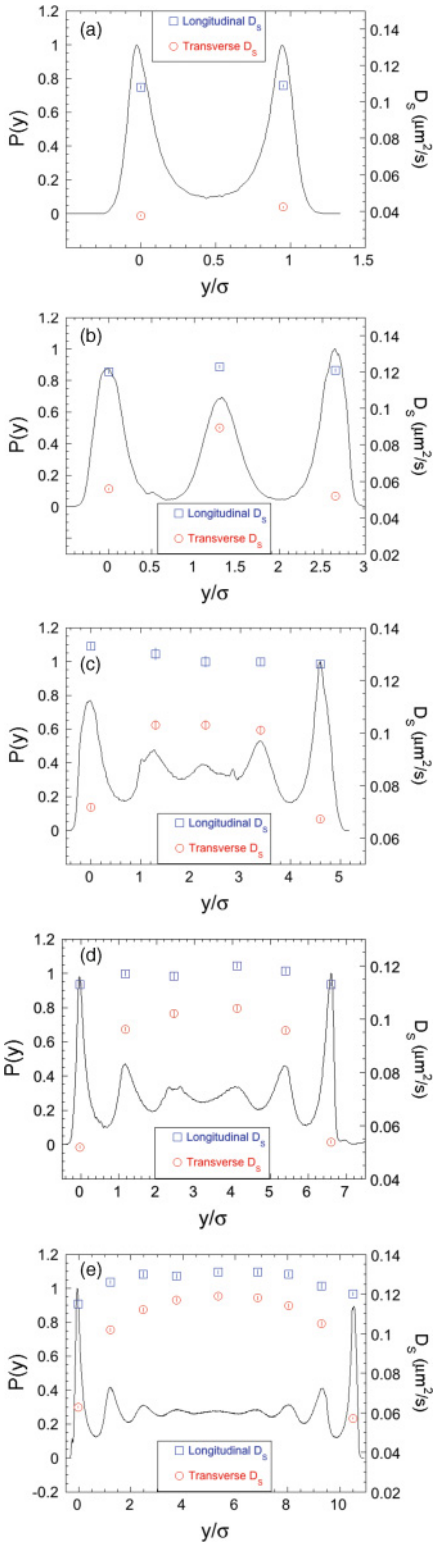

FIG. 2. (Color online) Samples of the experimental data for ribbon channels with widths of (a) 5 μm, (b) 8 μm, (c) 11 μm, (d) 14 μm, and (e) 20 μm, all with packing fraction $\phi \approx 0.4$. The figure shows a superposition of the transverse density profile in the ribbon channel and the single-particle diffusion coefficients along and perpendicular to the strata of the transverse density distribution. Error bars are shown; the error per point is typically smaller than the size of the data point displayed.

difference is only on the order of 2%–5% but is consistent for all channels.

(5) At the largest packing fraction studied, $\phi \approx 0.42$, as the ribbon width is increased, there is a weak increase in the central stratum value of the ratio of the single-particle transverse to longitudinal diffusion coefficients.

As reported previously, in a q1D colloid suspension, the hydrodynamic interaction between particles decays exponentially with scale length w, and two body hydrodynamic interactions remain dominant up to high particle density [10]. In a q2D colloid suspension confined between two hard walls with a small separation $H \sim \sigma$, the far field flow induced by the motion of a colloid particle has a momentum monopole contribution that is cut off by the boundary conditions at distances larger than the confinement width H, and a mass dipole contribution that decays as $(H/r)^2$, with the anisotropy of the dipolar flow field responsible for the negative sign of the coupling that affects the transverse pair diffusion coefficient [11].

Observation 1 clearly implies that the single-particle diffusion coefficient in the ribbon channel retains at least some q1D characteristic behavior in all of the systems studied, and observations 4 and 5 imply that the approach to q2D behavior is slow but noticeable. A sampling of the particle trajectories, such as shown in Fig. 4, reveals that there are very few exchanges of particles between strata even when the instantaneous particle displacements transverse to the average stratum midline are substantial. We note that the trajectories shown in Fig. 4 are 5-s long, much longer than the time interval of 0.18 s, used to calculate the short-time diffusion coefficients we report. Figure 4 shows that, on the time scale of interest, the strata deform and remain distinct, thereby restricting the magnitude of the transverse particle displacement relative to the longitudinal particle displacement.

This paper has focused attention on the transition from q1D to q2D behavior in dense colloid suspensions wherein both excluded volume and hydrodynamic interaction effects are important. In a dense suspension, because of the complex fluid flows generated by the interaction between the boundary conditions imposed by both the walls and any instantaneous configuration of impenetrable particles, parsing these contributions is difficult. In contrast, the influence of a nearby wall on the hydrodynamic interaction with an otherwise isolated spherical particle is well understood. Theoretical and experimental studies [12,13] (and references therein) show that both diffusion coefficients of an isolated particle perpendicular to a wall and parallel to a wall are reduced relative to that in the bulk liquid. At a distance from one wall of one particle radius, the perpendicular diffusion coefficient is reduced to zero, and the parallel diffusion coefficient is reduced to less than 0.4 of the value in the bulk liquid. The diffusion coefficients return to 0.8 of the bulk value only at distances from the wall of about six and three particle radii, respectively. The effect on isolated particle diffusion of several walls is tolerably accounted for by a linear superposition of the effects of each wall [13]. From observations 2 and 3, it is clear that our data do not follow the theoretical predictions for the wall-drag effect on isolated particles.

A full theoretical analysis of the influence of the density of the suspension on the single-particle diffusion coefficients

TABLE I. Single-particle longitudinal and transverse diffusion coefficients in ribbon channels with widths 8, 11, 14, and 20 μm, for several packing fractions.

Packing fraction	Stratum	D_{SL} ($\mu m^2/s$)	D_{ST} ($\mu m^2/s$)	D_{ST}/D_{SL}
8-μm channel				
0.18	1	0.177 ± 0.002	0.105 ± 0.002	0.59
0.18	2	0.187 ± 0.003	0.150 ± 0.003	0.80
0.18	3	0.185 ± 0.003	0.116 ± 0.002	0.63
0.26	1	0.153 ± 0.001	0.078 ± 0.001	0.51
0.26	2	0.161 ± 0.002	0.131 ± 0.001	0.81
0.26	3	0.158 ± 0.001	0.074 ± 0.001	0.47
0.43	1	0.120 ± 0.001	0.056 ± 0.001	0.47
0.43	2	0.123 ± 0.001	0.090 ± 0.001	0.73
0.43	3	0.121 ± 0.001	0.052 ± 0.001	0.43
11-μm channel				
0.11	1	0.188 ± 0.005	0.122 ± 0.004	0.65
0.11	2	0.202 ± 0.004	0.167 ± 0.004	0.83
0.11	3	0.205 ± 0.004	0.179 ± 0.003	0.87
0.11	4	0.194 ± 0.004	0.142 ± 0.003	0.73
0.40	1	0.122 ± 0.001	0.059 ± 0.001	0.48
0.40	2	0.127 ± 0.001	0.102 ± 0.001	0.80
0.40	3	0.131 ± 0.001	0.110 ± 0.001	0.84
0.40	4	0.129 ± 0.002	0.103 ± 0.001	0.80
0.40	5	0.123 ± 0.001	0.068 ± 0.001	0.55
0.42	1	0.133 ± 0.001	0.072 ± 0.001	0.54
0.42	2	0.130 ± 0.002	0.103 ± 0.002	0.79
0.42	3	0.127 ± 0.002	0.103 ± 0.002	0.81
0.42	4	0.127 ± 0.001	0.101 ± 0.001	0.80
0.42	5	0.126 ± 0.001	0.067 ± 0.001	0.53
14-μm channel				
0.21	1	0.164 ± 0.002	0.116 ± 0.002	0.71
0.21	2	0.170 ± 0.002	0.149 ± 0.002	0.88
0.21	3	0.170 ± 0.002	0.153 ± 0.002	0.90
0.21	4	0.165 ± 0.002	0.141 ± 0.002	0.85
0.21	5	0.157 ± 0.002	0.101 ± 0.002	0.64
0.25	1	0.160 ± 0.002	0.106 ± 0.001	0.66
0.25	2	0.165 ± 0.002	0.140 ± 0.002	0.85
0.25	3	0.162 ± 0.003	0.139 ± 0.003	0.86
0.25	4	0.164 ± 0.003	0.141 ± 0.002	0.86
0.25	5	0.162 ± 0.002	0.135 ± 0.002	0.83
0.25	6	0.155 ± 0.002	0.097 ± 0.001	0.63
0.44	1	0.113 ± 0.001	0.052 ± 0.001	0.46
0.44	2	0.117 ± 0.001	0.096 ± 0.001	0.82
0.44	3	0.116 ± 0.001	0.102 ± 0.001	0.88
0.44	4	0.120 ± 0.001	0.104 ± 0.001	0.87
0.44	5	0.118 ± 0.001	0.096 ± 0.001	0.81
0.44	6	0.113 ± 0.001	0.054 ± 0.001	0.48
20-μm channel				
0.17	1	0.150 ± 0.002	0.095 ± 0.002	0.63
0.17	2	0.160 ± 0.002	0.136 ± 0.003	0.85
0.17	3	0.162 ± 0.002	0.146 ± 0.003	0.90
0.17	4	0.163 ± 0.002	0.149 ± 0.002	0.91
0.17	5	0.164 ± 0.004	0.141 ± 0.003	0.86
0.17	6	0.164 ± 0.003	0.143 ± 0.003	0.87
0.17	7	0.164 ± 0.002	0.140 ± 0.003	0.85
0.17	8	0.154 ± 0.003	0.098 ± 0.002	0.64
0.32	1	0.139 ± 0.002	0.081 ± 0.001	0.58
0.32	2	0.155 ± 0.002	0.128 ± 0.001	0.83

TABLE II. (*Continued*)

Packing fraction	Stratum	D_{SL} ($\mu m^2/s$)	D_{ST} ($\mu m^2/s$)	D_{ST}/D_{SL}
20-μm channel				
0.32	3	0.157 ± 0.002	0.139 ± 0.001	0.89
0.32	4	0.157 ± 0.001	0.143 ± 0.001	0.91
0.32	5	0.151 ± 0.002	0.138 ± 0.001	0.91
0.32	6	0.156 ± 0.002	0.132 ± 0.002	0.85
0.32	7	0.155 ± 0.002	0.130 ± 0.001	0.84
0.32	8	0.148 ± 0.001	0.082 ± 0.001	0.55
0.41	1	0.115 ± 0.001	0.063 ± 0.001	0.55
0.41	2	0.126 ± 0.001	0.102 ± 0.001	0.81
0.41	3	0.130 ± 0.001	0.112 ± 0.001	0.86
0.41	4	0.129 ± 0.001	0.117 ± 0.001	0.91
0.41	5	0.131 ± 0.001	0.119 ± 0.001	0.91
0.41	6	0.131 ± 0.001	0.118 ± 0.001	0.90
0.41	7	0.130 ± 0.001	0.114 ± 0.001	0.88
0.41	8	0.124 ± 0.001	0.105 ± 0.001	0.85
0.41	9	0.120 ± 0.001	0.057 ± 0.001	0.48

parallel and perpendicular to a wall is not available. However, it is reasonable to expect that the complex fluid flows needed to satisfy the zero slip boundary condition on the surfaces of all particles in the system will severely alter the particle motion. A qualitative description of how the presence of other particles in a dense colloid suspension influences the dependence of the one-particle diffusion coefficient on separation from a wall has been provided by Michailidou *et al*. [8]. Assuming that particle-wall and particle-particle near field hydrodynamic interactions are the same because they have the same singular behavior near contact, in a high-density suspension, a particle cannot distinguish between a near neighbor particle and the wall, thereby greatly reducing the dependence of the one-particle diffusion coefficient on separation from the wall. Indeed, evanescent light scattering studies of colloid particle

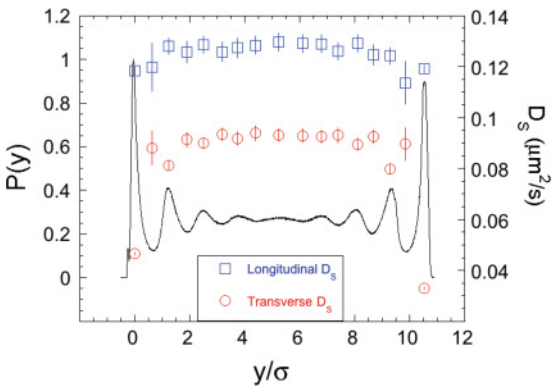

FIG. 3. (Color online) The single-particle diffusion coefficients in the 20-μm channel with packing fraction $\phi \approx 0.41$ along and perpendicular to equal width strata centered on the maxima and minima of the distribution of the transverse density distribution. Note that both the single-particle longitudinal and the transverse diffusion coefficients are sensibly the same for strata centered on minima and maxima of the density distribution, except for the strata closest to the walls of the channel. Error bars are shown; the error per point is typically smaller than the size of the data point displayed.

motion near a wall in a 3D system [7,8] show that, as the concentration of colloid particles increases, the effect of the wall on the diffusion coefficient decreases. And a confocal microscopy study of a dense q2D colloid suspension between hard walls [9] finds that the diffusion coefficient for motion parallel to the wall is sensibly independent of distance from the wall.

In the experiments reported in this paper, a colloid particle is always very close to one wall (the floor of the cell) and to many other particles, and the sidewall heights are only about two particle diameters. Extrapolating the observations relevant to 3D systems to the ribbon channel experiments, we expect that, if there is one particle in the ribbon channel, only motion parallel to the floor of the channel is possible, and that if the zero slip and impenetrability boundary conditions at the sidewalls are dominant despite the limited wall height, the expected transverse and longitudinal diffusion coefficients of an isolated colloid particle in a ribbon channel will vary strongly across the channel, unlike what we observe for a dense suspension in a ribbon channel. The qualitative argument offered by Michailidou *et al*. is equally applicable to colloid motion in 3D near a wall and to colloid motion in a ribbon channel. We conclude that excluded volume and the associated structural and lubrication effects grossly alter the hydrodynamic interactions and render the one-particle diffusion coefficient sensibly independent of particle-wall separation.

It is arguable that observation 3 is the least expected of the results, since the strata show substantial differences in their local densities as the ribbon width and colloid concentration are changed. In a bulk suspension, the diffusion coefficient is a strong function of the colloid density, and a conventional local density representation of the properties of the stratified suspension in the ribbon channel leads to the expectation of a corresponding variation with stratum density of the diffusion coefficient. We interpret observation 3 using the Fischer-Methfessel representation of the local density in an inhomogeneous fluid. Fischer and Methfessel pointed out that,

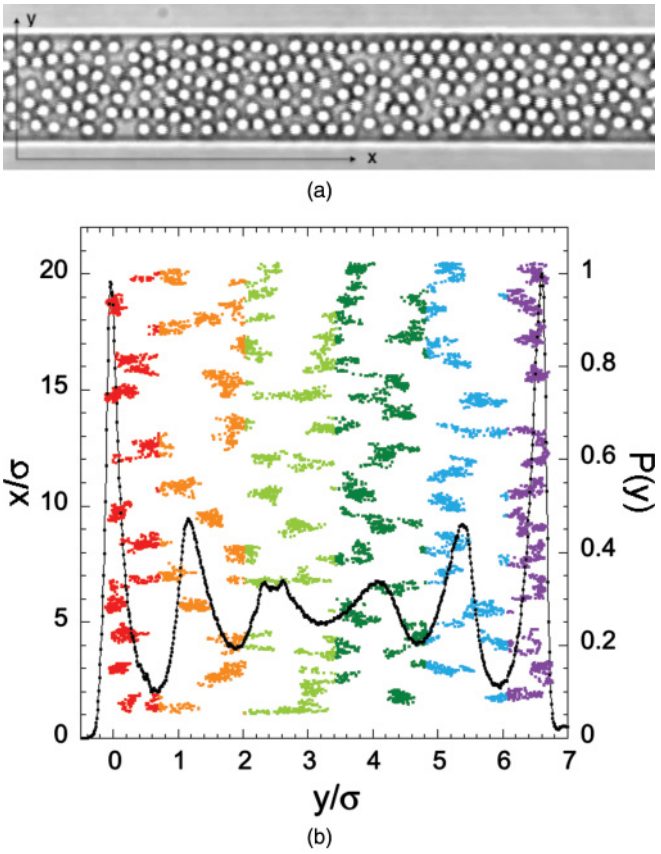

FIG. 4. (Color online) (a) Image of the 14-μm ribbon channel with packing fraction $\phi \approx 0.44$. (b) Transverse trajectories of the colloid particles in the channel pictured above as a function of position along the channel. The data were collected over a 5-s interval. Different strata are pictured in different colors (gray levels) with the density distribution $P(y)$ included as a guide to the eye.

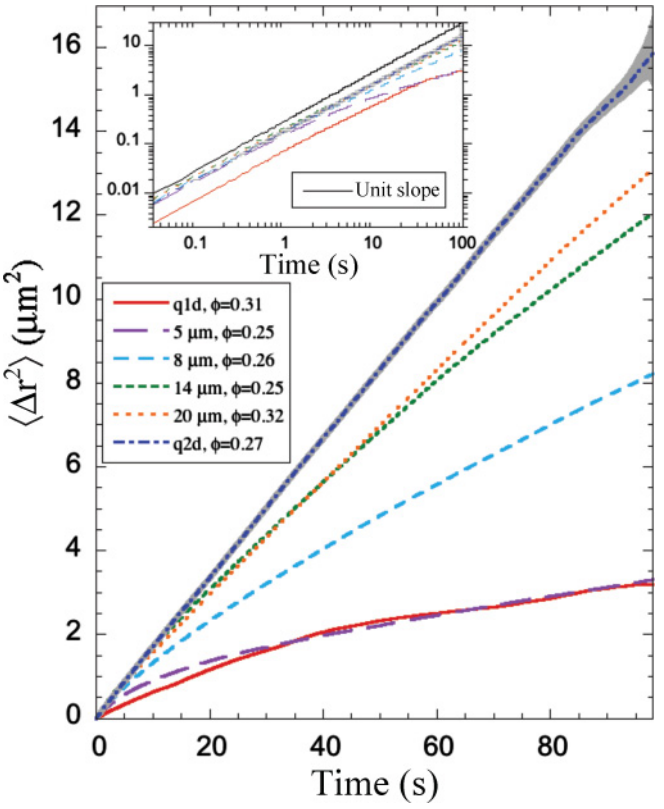

FIG. 5. (Color online) Mean squared displacement as a function of time in several ribbon channels and the q2D colloid suspension ($\phi \approx 0.27$). The error bars for all data sets, except for q2D, are less than the width of the lines. Error bars for the q2D data set are shown.

to sustain a density gradient in an inhomogeneous liquid, there must be a balancing force that is not captured by representing the local density as a point function [14]. They showed that, for lowest order, the source of the force was, typically, interaction with nearest neighbors of a molecule and, therefore, defined the local density as an average over a volume with a radius of one particle diameter. It has been shown that this approximation provides a good description of the pair correlation function in the inhomogeneous transition region in the liquid-vapor interface [15]. The application for our results follows from the observation that at the colloid suspension densities we have studied the hydrodynamic interactions between colloid particles in q1D and q2D geometries are determined by the pair-correlation function. Applying the Fischer-Methfessel approximation to the description of our system implies defining the local density by averaging over neighboring strata, thereby sensibly removing the density variation of the pair-correlation function and the density variation of the friction coefficient.

Finally, we address question 3 raised in Sec. I. In Fig. 5, we display the mean square displacement of a particle as a function of time for colloid suspensions with $\phi \approx 0.27$ in a q1D channel, ribbon channels with widths of 5–20 μm, and a q2D geometry. These mean squared displacements were calculated for all particles across the full width of the ribbon channel. In all of these systems, the mean square displacement increases linearly with time for short time, but only for the q2D geometry is it linear at long time. The data for the q1D channel clearly show a deviation in the mean square displacement from a linear dependence on time and an approach to the predicted dependence on the square root of time. The mean square displacement data for the 5–20-μm channels show deviations from a linear dependence on time that are similar to that observed in q1D but decrease as the channel width increases. Note that the long-time dependence of the mean square displacement for a particle in the widest ribbon channel still deviates from the q2D linear time dependence. The effect of the confinement is clearly shown as the width of the channel is reduced.

IV. CONCLUSION

We have examined the behavior of single-particle short-time diffusion in a dense colloid fluid confined in a ribbon channel in which the transverse density distribution is stratified. By addressing the questions raised in Sec. I, we see again that this stratified dense liquid exhibits characteristics of both q1D and q2D fluids, depending on the length scale over which the properties are probed. This conclusion confirms that reached in our previous papers on the equilibrium structural properties, via measurements of

the pair-correlation functions, and hydrodynamic coupling, via measurements of the pair-diffusion coefficients, of the same colloid particles in the same ribbon channels. The most striking result of this paper is that, when measured along individual strata peaks or valleys, the longitudinal diffusion coefficients are essentially uniform across the width of the channel, whereas, the transverse diffusion coefficients are sensitive to the variation in the density distribution and the wall-drag effect as observed in a dilute bulk colloid fluid. The findings in this paper and our previous papers should provide useful insight into the phenomena observed on different length scales in biological structures and/or microfluidic applications that are intermediate between q1D and q2D.

ACKNOWLEDGMENTS

The research reported in this paper was supported by the NSF funded MRSEC Laboratory (Grant No. DMR-0820054) at the University of Chicago. B.L. also acknowledges support for this research from ChemMatCARS (NSF-DOE, Grant No. CHE-0822838).

[1] C. Bechinger, Curr. Opin. Colloid Interface Sci. **7**, 204 (2002).
[2] H. Diamant, J. Phys. Soc. Jpn. **78**, 041002 (2009).
[3] T. M. Squires and S. R. Quake, Rev. Mod. Phys. **77**, 977 (2005).
[4] S. A. Rice, Chem. Phys. Lett. **479**, 1 (2009).
[5] S. Novikov, S. A. Rice, B. Cui, H. Diamant, and B. Lin, Phys. Rev. E **82**, 031403 (2010).
[6] T. R. Stratton, S. Novikov, R. Qato, S. Villarreal, B. Cui, S. A. Rice, and B. Lin, Phys. Rev. E **79**, 031406 (2009).
[7] P. Holmqvist, J. K. G. Dhont, and P. R. Lang, Phys. Rev. E **74**, 021402 (2006).
[8] V. N. Michailidou, G. Petekidis, J. W. Swan, and J. F. Brady, Phys. Rev. Lett. **102**, 068302 (2009).
[9] C. R. Nugent, K. V. Edmond, H. N. Patel, and E. R. Weeks, Phys. Rev. Lett. **99**, 025702 (2007).
[10] B. Cui, H. Diamant, and B. Lin, Phys. Rev. Lett. **89**, 188302 (2002).
[11] B. Cui, H. Diamant, B. Lin, and S. A. Rice, Phys. Rev. Lett. **92**, 258301 (2004).
[12] J. Happel and H. Brenner, *Low Reynolds Number Hydrodynamics* (Kluwer Academic, Dordrecht, 1983).
[13] B. Lin, J. Yu, and S. A. Rice, Phys. Rev. E **62**, 3909 (2000).
[14] J. Fischer and M. Methfessel, Phys. Rev. A **22**, 2836 (1980).
[15] J. Harris and S. A. Rice, J. Chem. Phys. **86**, 5731 (1987).